

Complete path entanglement of two photons

Alessandro Rossi,¹ Giuseppe Vallone,^{1,2,*} Francesco De Martini,^{1,2,3,*} and Paolo Mataloni^{1,2,*}

¹ *Dipartimento di Fisica della Sapienza Università di Roma, Roma, 00185 Italy*

² *Consorzio Nazionale Interuniversitario per le Scienze Fisiche della Materia, Roma, 00185 Italy*

³ *Accademia Nazionale dei Lincei, via della Lungara 10, Roma 00165, Italy*

(Dated: November 7, 2018)

We present a novel optical device based on an integrated system of microlenses and single mode optical fibers. It allows to send in many directions two photons generated by spontaneous parametric down conversion. By this device multiqubit entangled states and/or multilevel qudit states of two photons, encoded in the longitudinal momentum degree of freedom, are created. The multipath photon entanglement realized by this device is expected to find important applications in modern quantum information technology.

PACS numbers: 42.65.Lm, 42.79.Ry, 42.50.Dv

Keywords: parametric down conversion, multiqubit entanglement, microlens

By entangling two photons in a high-dimension Hilbert space many important tasks of quantum information are performed. These deal with a complete analysis of Bell states [1, 2, 3] and novel protocols of superdense coding [4], the possibility of enhancing the security of some cryptographic protocols [5, 6], and a fast, high-fidelity one-way quantum computation [7], [8, 9, 10, 11], besides advanced tests of quantum nonlocality [12, 13, 14, 15].

Multidimensional entangled states of two photons have been realized in the last years by creating both qudit states and hyperentangled states. In the former each particle belongs to a d -level quantum system, in the latter the particles are entangled in many degree of freedoms (DOF's). Since a qudit, with $d = 2^N$, is equivalent to N qubits, two-entangled qudits with $d = 2^N$ are equivalent to a hyperentangled state, enabling the entanglement of two particles in N DOF's. Polarization, time bin and spatial entanglement have been used to engineer qudits with $d = 3$ [6, 16], $d = 4$ [17] and even $d = 8$ [18]. At the same time, hyperentangled states have been produced by adopting in different combinations polarization, longitudinal momentum and orbital angular momentum DOF's, besides time-bin entanglement [2, 19, 20, 21, 22].

In this paper we present the first experimental realization of a quantum state of two photons entangled in many optical paths. It is based on the spontaneous parametric down conversion (SPDC) emission of a Type I phase-matched nonlinear (NL) crystal operating under the continuous wave (cw) excitation of a laser at wavelength (wl) λ_p . In these conditions, the degenerate signal (s) and idler (i) photons, are generated with uniform probability distribution, at wl $\lambda_s = \lambda_i = 2\lambda_p$, over a continuum of correlated \mathbf{k} -modes belonging to the lateral surface of a cone. Usually, no more than two correlated spatial modes are used in experiments based on Type I crystals, hence the main part of SPDC radiation is lost. By exploiting the continuum of \mathbf{k} -mode emission of the

Type I crystal a high-dimension entangled state can be created [23]. Indeed, a very large number of qubits are in principle available by this geometry. However, a successful realization of this idea strongly depends on the possibility to overcome the practical difficulties represented by independently collecting and manipulating the SPDC radiation belonging to a large number of \mathbf{k} -modes.

The device realized in this experiment allows the efficient coupling of SPDC photon pairs travelling along a large number of \mathbf{k} -modes into a bundle of single mode optical fibers by an integrated system of microlenses. Four pairs of correlated \mathbf{k} -modes were selected to generate a 4-qubit hyperentangled state (or equivalently two entangled ququarts, i.e. qudits with $d = 4$) encoded in the longitudinal momentum of the photons. The path-entanglement existing over the entire set of optical modes collected by the system were also characterized in the experiment.

Figure 1a) shows the annular section of the cone, where four pairs of correlated modes are selected. It is divided in two half-rings, respectively corresponding to the Alice (A) and Bob (B) side. The generated state can be expressed by two maximally entangled qudits $|\phi^{(d)}\rangle_k = \sum_{j=1}^d \frac{1}{\sqrt{d}} (e^{i\phi_j} |j\rangle_A |j\rangle_B)$ with $d = 4$ and ϕ_j corresponding to the phase of the j mode pair. The modes $|1\rangle_A, \dots, |4\rangle_A$ belonging to the A side can be relabelled respectively as $|E, \ell\rangle_A, |I, \ell\rangle_A, |I, r\rangle_A$ and $|E, r\rangle_A$, where ℓ (r) and E (I) refer to the left (right) and external (internal) emission modes (see Figure 1b)). These modes are respectively correlated to the B emission modes $|E, r\rangle_B, |I, r\rangle_B, |I, \ell\rangle_B$ and $|E, \ell\rangle_B$, labelled as $|1\rangle_B, \dots, |4\rangle_B$ in Figure 1a). The radiation travelling along the eight modes then represents a 4-qubit hyperentangled state:

$$\frac{1}{\sqrt{2}} (|\ell\rangle_A |r\rangle_B + |r\rangle_A |\ell\rangle_B) \otimes \frac{1}{\sqrt{2}} (|I\rangle_A |I\rangle_B + |E\rangle_A |E\rangle_B) \quad (1)$$

Two qubits are thus encoded in each photon, namely the $\ell - r$ qubit and the $E - I$ qubit. This geometry allows in principle the creation of a hyperentangled or

*URL: <http://quantumoptics.phys.uniroma1.it/>

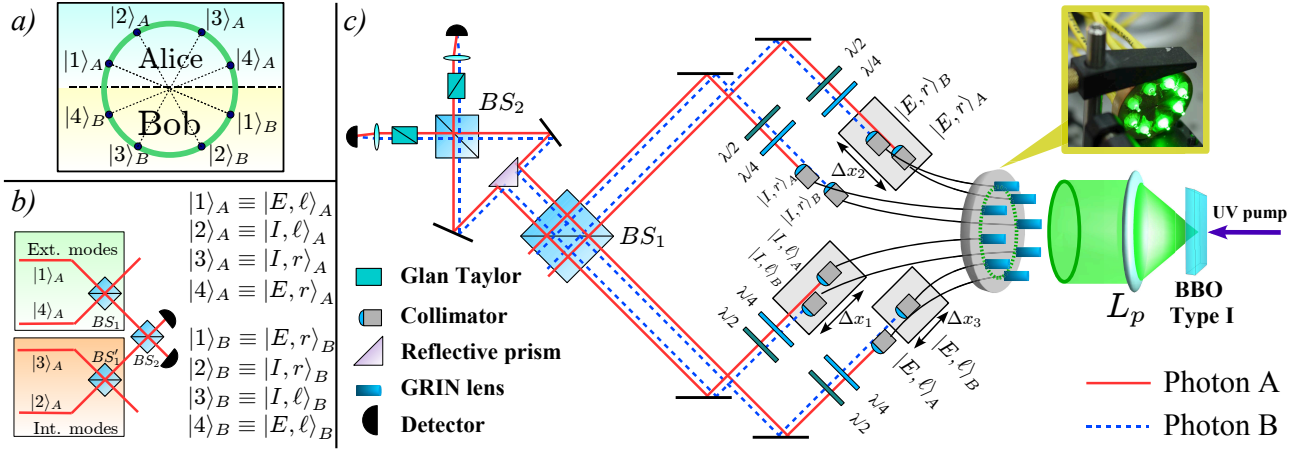


FIG. 1: *a)* Labelling of the eight SPDC collected modes, linked two by two by the dashed lines. Photon *A* (*B*) is collected in four modes $|1\rangle_j$, $|2\rangle_j$, $|3\rangle_j$ or $|4\rangle_j$ ($j = A, B$). These are relabelled as shown in *b)* to emphasize the equivalence existing between a ququart ($d = 4$) and two qubits. *b)* Scheme needed for the measurement of the two qubits of photon *A*. Beam splitters BS_1 and BS_1' measure the $\ell - r$ qubit, the second beam splitter BS_2 measures the $E - I$ qubit. An identical scheme is needed for photon *B*. *c)* Experimental setup: a Type I 2mm thick β -barium-borate (BBO) crystal, cut at $\theta = 51.4$ deg is shined by a single longitudinal mode MBD-266 Coherent laser ($P = 120mW$, $\lambda_p = 266nm$) with vertical (*V*) polarization. Photon pairs are generated with horizontal (*H*) polarization along correlated directions belonging to the external surface of the SPDC cone at $wl \lambda_s = \lambda_i = 532nm$. The 8 GL-SMF system collects and injects the SPDC radiation into a chained interferometer. The photon *A* (*B*) path is indicated by a continuous red (dashed blue) line. By this scheme BS_1 acts for both photons as BS_1 and BS_1' of side *b)*. Path delay between the different modes is set to zero by varying Δx_i ($i = 1, 2, 3$). Waveplates $\lambda/4$ and $\lambda/2$ allow photon polarization restoration after transmission through SMF's. Inset: picture of the 8-GL system. The whole apparatus is closed within an insulating box and thermally stabilized in order keep constant the phase of the state.

qudit entangled state with a very large value of d , as said. However, it is worth to remember that the number of \mathbf{k} -modes doesn't scale linearly with the number of qubits. Indeed, 2^N \mathbf{k} -modes per photon must be selected within the emission cone of the crystal to encode N qubits in each photon. On the other hand, since a qudit, with $d = 2^N$, is equivalent to N qubits, the number of modes scales linearly with the size d of the state.

The device allowing to collect the SPDC radiation into a set of single mode fibers consists of two parts:

i) A positive lens L_p (focal length $f = 9.5cm$), located at a distance f from the BBO, transforms the SPDC conical emission into a cylindrical one with transverse diameter $D = 12mm$.

ii) An integrated system of eight equal silver exchanged graded-index lenses (GL's), regularly spaced along a D -diameter annular ring, intercepting the degenerate SPDC ring.

Each GL (Grintech, mod. GT-LFRL-100-025-50-NC (532), length $l = 2.381mm$, diameter $d = 1.0mm$, numerical aperture $N.A. = 0.5$), allowing to focus the SPDC radiation on its output face, was glued to the input of a pre-aligned single-mode fiber (SMF). More than 50% efficiency was measured for each GL-SMF system and the overall *coincidences* / *singles* ratio was typically larger than 10%. The GL-SMF systems were glued inside an especially prepared 8-hole brass screen in order to realize a single integrated device (see inset of Figure 1c). On this purpose, the position of each GL-SMF pair was

optimized by coincidence detection of the corresponding correlated \mathbf{k} -modes. Nearly $7 \cdot 10^3$ *coinc*/s were measured for each mode pair over a bandwidth $\Delta\lambda = 4.5nm$.

The entanglement existing between the four pairs of modes was characterized by the interferometric apparatus sketched in Figure 1c). Indistinguishability between the four modes on which each photon can be emitted is achieved by the sequence of beam splitters of Figure 1b). In the actual chained interferometer setup used in the experiment the \mathbf{k} -modes corresponding to photons *A* or *B*, are matched on the up and down side of a common 50:50 beam splitter (BS_1). Here temporal mode matching is realized by fine adjustment of three optical paths by spatial delays Δx_1 , Δx_2 , Δx_3 . SPDC radiation coming out of each SMF enters into the input port of a symmetric beam splitter BS_1 . Precisely, mode $|I, \ell\rangle_A$ ($|E, \ell\rangle_A$) interfere with mode $|I, r\rangle_A$ ($|E, r\rangle_A$). The same happens with the corresponding *B* modes. This interference is due to the spatial and temporal indistinguishability obtained by changing the delay Δx_1 (Δx_3) on BS_1 between the $|I, r\rangle_A |I, \ell\rangle_B$ ($|E, \ell\rangle_A |E, r\rangle_B$) and $|I, \ell\rangle_A |I, r\rangle_B$ ($|E, r\rangle_A |E, \ell\rangle_B$) events. Note that the interference condition on BS_1 is independently achieved for the internal and external mode sets. This operation acts as a measurement on the $\ell - r$ qubit since the output ports of the BS_1 are respectively $\frac{1}{\sqrt{2}}(|\ell\rangle_j \pm e^{i\alpha_j} |r\rangle_j)$ (with $j = A$ or $j = B$) regardless of the value of the $E - I$ qubit.

In order to measure the $I - E$ qubit and thus test the path entanglement occurring over the entire set of

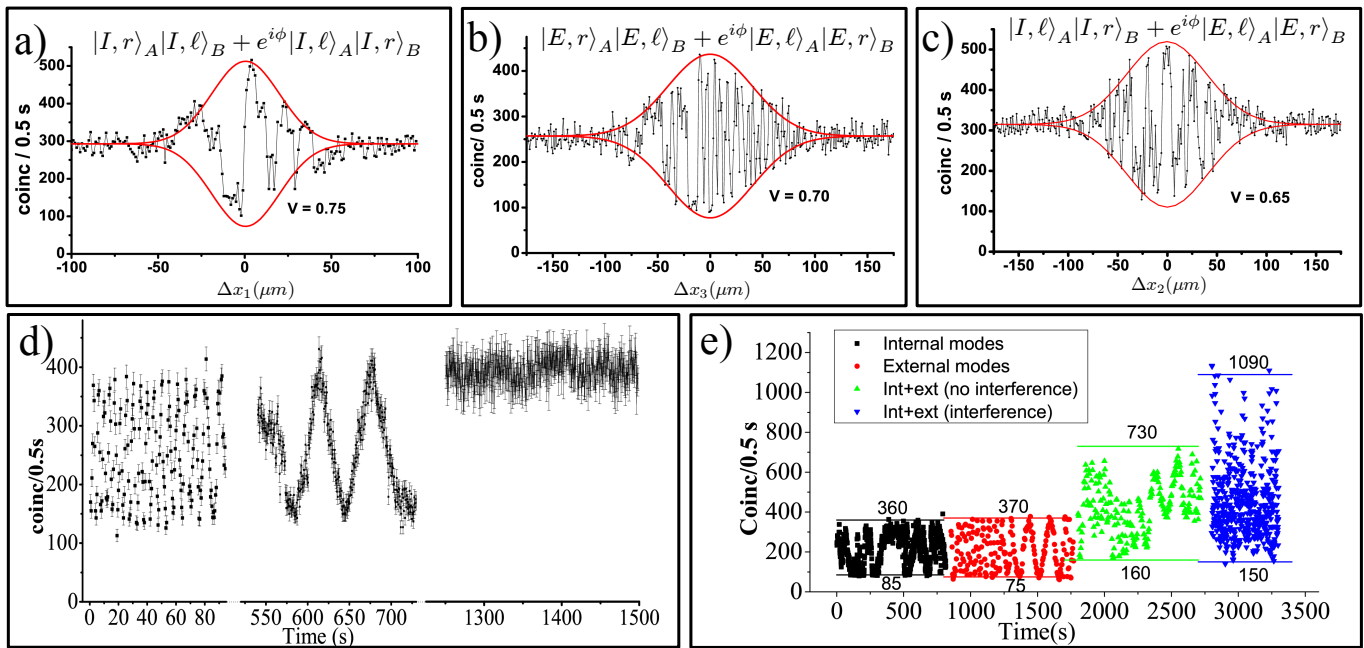


FIG. 2: Interference patterns obtained by spatial superposition of the internal (a) and external modes (b) on BS_1 as a function of delays Δx_1 and Δx_3 . c): "Hybrid" interference condition, obtained as a function of Δx_2 by spatial superposition on BS_2 of the internal with the external modes. All the measurements are performed without temperature stabilization of the fiber apparatus. d): Effect of temperature stabilization for internal mode interference ($\Delta x_1 = 0$). Coincidence counts are reported as a function of time T , starting from the switching on of the stabilization apparatus ($T = 0$). e): Coincidence counts demonstrating the complete interference existing between the four pairs of modes. The first two experimental data show the coincidence counts measured when the internal (visibility $V \sim 62\%$) and external ($V \sim 66\%$) modes are separately considered. The data are taken under interference condition on BS_1 . The third series of data are taken by considering all the four pairs of modes, but without interference on BS_2 (i.e. by setting $\Delta x_1 = \Delta x_3 = 0$ and $\Delta x_2 \neq 0$). Here the measurements are affected by phase fluctuations of the first ($\ell - r$ qubit) interferometer. The last data show the experimental coincidence counts measured when all modes interfere (i.e. with $\Delta x_1 = \Delta x_2 = \Delta x_3 = 0$). The upper bound of coincidence counts (1090) compared to the maximum obtained in case of no interference (730) corresponds to a total visibility $V \sim 50\%$.

\mathbf{k} -modes we need to create interference on the BS_2 . This corresponds to make indistinguishable the four event $|1\rangle_A |1\rangle_B$, $|2\rangle_A |2\rangle_B$, $|3\rangle_A |3\rangle_B$ and $|4\rangle_A |4\rangle_B$ when a coincidence is detected.

The interference is observed between the output modes of the first beam splitter BS_1 , i.e. by superposing the internal and external mode sets on BS_2 . Let's consider the right output port of BS_1 in Figure 1c). There are two modes, both for Alice and Bob sides, each coming from the internal or external part of the first interferometer. Both photons come from the left or right BS_2 input, if they belong to the internal or external modes, respectively. Thus, changing the path delay of the internal or external modes, it is possible to achieve temporal indistinguishability on BS_2 . This can be achieved by simultaneously varying Δx_2 and Δx_3 . Precisely, for any $\Delta x_2 = \delta L$ and $\Delta x_3 = 2\delta L$, we simultaneously keep the interference on BS_1 and change the delay of the external modes. In this way we can simultaneously achieve interference of both BS_1 and BS_2 . Fine alignment on both BS_1 and BS_2 allowed accurate phase tuning of the entangled state. In the experiment phase stability was achieved by mechanical stabilization of the interferomet-

ric setup and by thermally stabilizing the fiber setup.

The interference patterns shown in Figures 2a) and 2b), obtained by respectively varying Δx_1 and Δx_3 , demonstrate the existence of path entanglement (on BS_1), both for the internal and external mode sets. The interference patterns are affected by phase instabilities due to the incremental steps of Δx_1 and Δx_2 . This is less evident in Figure 2a) where the phase is a low varying function of Δx_1 (mainly dependent on the single fiber stress) which corresponds to a simultaneous variation of both the optical delays of modes $|I, \ell\rangle_A$ and $|I, \ell\rangle_B$ [19]. For the same reason the FWHM duration of the interference pattern of Figure 2b) doubles the one of Figure 2a).

The two results demonstrate interference on BS_1 and hence the separate entanglement for the internal and external modes, but not necessarily the complete path entanglement over the entire set of modes. This is demonstrated by the third interference pattern of Figure 2c) occurring on BS_2 between $|I, \ell\rangle_A |I, r\rangle_B$ and $|E, \ell\rangle_A |E, r\rangle_B$, and obtained by varying Δx_2 .

The effect of temperature stabilization on the internal mode interference is demonstrated in Figure 2d) show-

ing the number of coincidences as a function of time, for $\Delta x_1 = 0$. Starting from time $T = 0$, i.e. from the instant of turning on the stabilization apparatus, the phase first changes rapidly determining a fast variations of the coincidence counts. After 10 minutes the phase changes more slowly ($\sim 2\pi/\text{minute}$), while after 20 minutes it is almost completely stabilized.

As a final demonstration of the complete entanglement we compare in Figure 2e) the signal oscillations obtained for $\Delta x_1 = \Delta x_2 = \Delta x_3 = 0$. We kept the system not stabilized in temperature such that the phase of the states is almost fixed in each acquisition data (0.5 s) but is varying during the different acquisitions. The first two oscillations respectively correspond to the separate internal and external interference, i.e. by keeping only the internal or external modes. The third oscillation corresponds to the coincidence counts for both internal and external modes without temporal superposition (and then interference) on the BS_2 . This must be compared with the fourth oscillation data obtained with $\Delta x_1 = \Delta x_2 = \Delta x_3 = 0$ that clearly shows multipath interference due to the complete indistinguishability of the four pairs of modes.

We have presented in this paper the first experimental realization of a multipath entanglement of two photons. The experiment was performed by collecting four pairs of correlated modes of the degenerate SPDC radiation emitted by a NL crystal cut for Type I phase matching. On this purpose we successfully realized an integrated system of eight GRIN lenses coupled to a corresponding set of single mode fibers. We tested the entanglement

generated over the entire SPDC conical emission of the crystal by using a specially developed chained-multipath-interferometer.

The novel device presented in this paper can be extended to an even larger of \mathbf{k} -modes by exploiting the continuum emission of the crystal and can be used together with an integrated optical circuit to realize miniaturized quantum optical networks of increasing complexity [24].

Besides multiqubit entanglement, this system can be successfully used in other quantum information processes. As an example, it can be adopted in the realization of a “quasi-deterministic” source of heralded single photons emitted along one half of the SPDC modes and triggered by the photons emitted along the other half of correlated modes [25]. The same device allows the efficient multiplexing transmission to many pairs of users and over long fiber distances of time-bin entanglement, which is not affected by thermal or mechanical fiber instabilities [26].

This device is a useful tool for an efficient generation and distribution of entanglement since it allows to maximize the emission of photon pairs for a given value of pump power. Other configurations can be used on this purpose, for instance those based on a sequence of mirrors and beam splitters or several nonlinear crystal, but at the price of a strong reduction of SPDC coincidences.

This work was supported by Finanziamento di Ateneo 06, Sapienza Università di Roma.

-
- [1] M. Barbieri, G. Vallone, P. Mataloni, and F. De Martini, *Phys. Rev. A* **75**, 042317 (2007).
 - [2] C. Schuck, G. Huber, C. Kurtsiefer, and H. Weinfurter, *Phys. Rev. Lett.* **96**, 190501 (2006).
 - [3] T.-C. Wei, J. T. Barreiro, and P. G. Kwiat, *Phys. Rev. A* **75**, 060305(R) (2007).
 - [4] J. T. Barreiro, T.-C. Wei, and P. G. Kwiat, *Nat. Phys.* **4**, 282 (2008).
 - [5] H. Bechmann-Pasquinucci and A. Peres, *Phys. Rev. Lett.* **85**, 3313 (2000).
 - [6] R. Thew, A. Acin, H. Zbinden, and N. Gisin, *Quantum Information and Computation* **4**, 93 (2004).
 - [7] H. J. Briegel and R. Raussendorf, *Phys. Rev. Lett.* **86**, 910 (2001). R. Raussendorf and H. J. Briegel, *ibid.* **86**, 5188 (2001).
 - [8] G. Vallone, E. Pomarico, P. Mataloni, F. De Martini, and V. Berardi, *Phys. Rev. Lett.* **98**, 180502 (2007).
 - [9] K. Chen *et al.*, *Phys. Rev. Lett.* **99**, 120503 (2007).
 - [10] G. Vallone, E. Pomarico, F. De Martini, and P. Mataloni, *Phys. Rev. Lett.* **100**, 160502 (2008).
 - [11] G. Vallone, E. Pomarico, F. De Martini, and P. Mataloni, *Laser Phys. Lett.* **5**, 398 (2008).
 - [12] D. Collins, N. Gisin, N. Linden, S. Massar, and S. Popescu, *Phys. Rev. Lett.* **88**, 040404 (2002).
 - [13] M. Barbieri, F. De Martini, P. Mataloni, G. Vallone, and A. Cabello, *Phys. Rev. Lett.* **97**, 140407 (2006).
 - [14] D. Kaszlikowski, P. Gnaniński, M. Żukowski, W. Miklaszewski, and A. Zeilinger, *Phys. Rev. Lett.* **85**, 4418 (2000).
 - [15] T. Yang *et al.*, *Phys. Rev. Lett.* **95**, 240406 (2005).
 - [16] G. Vallone, E. Pomarico, F. De Martini, P. Mataloni, and M. Barbieri, *Phys. Rev. A* **76**, 012319 (2007).
 - [17] E. V. Moreva, G. A. Maslennikov, S. S. Straupe, and S. P. Kulik, *Phys. Rev. Lett.* **97**, 023602 (2006).
 - [18] L. Neves *et al.*, *Phys. Rev. Lett.* **94**, 100501 (2005).
 - [19] M. Barbieri, C. Cinelli, P. Mataloni, and F. De Martini, *Phys. Rev. A* **72**, 052110 (2005).
 - [20] J. T. Barreiro, N. K. Langford, N. A. Peters, and P. G. Kwiat, *Phys. Rev. Lett.* **95**, 260501 (2005).
 - [21] C. Cinelli, M. Barbieri, R. Perris, P. Mataloni, and F. De Martini, *Phys. Rev. Lett.* **95**, 240405 (2005).
 - [22] W.-B. Gao *et al.*, preprint, [arXiv:0809.4277], (2008).
 - [23] M. Żukowski, A. Zeilinger, and M. A. Horne, *Phys. Rev. A* **55**, 2564 (1997).
 - [24] Politi, Cryan, Rarity, Yu, and O’Brien, *Science* **320**, 646 (2008).
 - [25] A. L. Migdall, D. Branning, and S. Castelletto, *Phys. Rev. A* **66**, 053805 (2002).
 - [26] J. Brendel, N. Gisin, W. Tittel, and H. Zbinden, *Phys. Rev. Lett.* **82**, 2594 (1999).